Mössbauer study of atomic order in Ni₃Fe. I. Determination of the long-range-order parameter

J. W. Drijver* and F. van der Woude

Solid State Physics Laboratory, Materials Science Center, University of Groningen, Groningen, The Netherlands

S. Radelaar

Technical Physics Department, Experimental Physics Laboratory, University of Utrecht, Utrecht, The Netherlands
(Received 13 December 1976)

By means of Mössbauer spectroscopy we studied the structural order in a series of stoichiometric Ni₃Fe foils, which had been given different heat treatments. The long-range-order parameter η was determined with an accuracy of ± 0.02 by analyzing the profiles of the outer lines of ^{57}Fe absorption spectra, recorded at room temperature. From the analysis it appeared that the hyperfine field at ^{57}Fe nuclei depends linearly on the numbers of iron atoms in the first and second neighboring shell, and that contributions from more distant atoms are negligible. Further anisotropic hyperfine interactions in Ni₃Fe are small. A comparison with η as determined from x-ray diffraction indicates that the wrongly placed atoms in partly ordered Ni₃Fe are distributed at random over the lattice sites.

I. INTRODUCTION

One of the early examples of what we nowadays call "materials engineering" is the development, since 1913, of the permalloys. The influence of atomic order on the magnetic properties of these fcc Ni-Fe alloys around the Ni₃Fe composition was understood much later.[1,2] In Ni₃Fe two factors have hampered the study of order-disorder processes. First, the reaction is extremely sluggish. Second, the usual diffraction techniques proved to be ineffective, due to the small change in lattice parameter upon ordering[3,4] (0.1%) and to the near equality of x-ray and neutron scattering factors for the two elements. For neutron diffraction this last problem has been overcome by the use of particular Ni isotopes,[5-7] but x-ray techniques have only recently been advanced so far that order parameters can be determined accurately.[8-10] Nevertheless information about the ordering behavior of Ni₃Fe was obtained, partly from diffraction experiments, but mainly from indirect methods such as dilatometry,[11] calorimetry,[12] or measurement of mechanical properties,[4,13,14] resistivity,[3,15] or magnetization.[3] Also transmission electron[16] and field-ion[17] microscopy have been employed.

At high temperatures iron can be dissolved in nickel up to 70 at.%, the Invar region. At lower temperatures the ordered alloys NiFe and Ni₃Fe are formed. Ordered Ni₃Fe has the L1₂ structure (Fig. 1). The ordering temperature, defined as the highest temperature at which an ordering reaction can be observed, lies near 770 K and shows a maximum at 27-at.% Fe.[11] The ordering is accompanied by a 5% increase in saturation magnetization[3] and an 8% increase in the ferromag-netic Curie temperature.[18] The hyperfine fields H_{hf} at the Ni and Fe nuclei also change upon ordering: The average value of $|H_{hf}|$ increases by 14% at Ni nuclei,[19,20] and decreases by 4% at Fe nuclei,[21,22] as measured with NMR or Mössbauer effect (ME) techniques. The recorded spectra show a structure which is attributed to local variations of H_{hf} at nuclei in different surroundings. These hyperfine field distributions have been employed earlier for the determination of order in Ni₃Fe.[20,21] We present here a more detailed analysis of ME spectra, taken at room temperature from a series of Ni₃Fe foils with varying long-range order.[23] We avoided some unnecessary simplifications (see Sec. III), and we also verified that the reaction proceeded homogeneously (see also the following paper). For comparison we determined the long-range order in several of the foils by means of x-ray diffraction.

II. EXPERIMENTAL PROCEDURES

A. Specimen preparation

Stoichiometric amounts of 5N Ni and Fe sponge were reduced in hydrogen and melted together in an alumina crucible by direct induction heating in vacuum. The ingots were homogenized at 1300 K in evacuated silica ampoules for one week. The
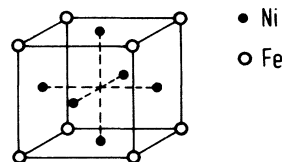
FIG. 1. L1₂ structure of ordered Ni₃Fe.

total weight loss was 0.12 Wt.%, so that the alloy is very near to its nominal composition. This was confirmed by a chemical analysis. Subsequently, the alloy was cold rolled to foils of about 35 μm thickness.

In order to investigate systematically the influence of order on the Mössbauer-line profiles, we prepared from two ingots two series of foils with increasing long-range order, hereafter called series A and B. The foils of each series were annealed together in a furnace in vacuum (10^{-4} Torr), first at 760 K, then stepwise at lower temperatures. During the annealing procedure the foils were succesively taken out of the furnace, which for this purpose was cooled down for a short time. From these foils, Mössbauer absorption spectra were recorded at room temperature, using the naturally present ^{57}Fe isotope.

B. Mössbauer and x-ray equipment

The Mössbauer spectrometer employed was of a conventional constant-acceleration type,[24] which gives two mirror spectra. For the velocity calibration we used the splitting of the outer lines from a natural-iron absorber (6 μm thickness) at 293 K: 10.625 mm sec^{-1} = 330 kOe. With the known positions of the six lines, a third-power fit of the velocity to the channel number was performed. The coefficients obtained were used in a spectrum-fitting program for linearization of the velocity scale. Then the two mirror spectra were added, resulting in improved statistics. In this way one also obtains a constant background, so that two parameters in the fitting procedure are eliminated. The spectra were least-squares fitted as a sum of Lorentzians.

Intensities of 100 and 200 Debye-Scherrer lines were measured with a Philips instrument, employing Co $K\alpha$ radiation, graphite diffracted-beam monochromator, proportional counter, pulse-height discriminator and step scanner. The intensity of a Debye-Scherrer line with indices hkl and reflection angle 2θ can be written[25]

$$I_{hkl} = CL(\theta)P(\theta, \theta_m)|F_{hkl}|^2 n_{hkl} D(\theta, T) .$$

The terms are defined as follows: C is an experimental constant; L the Lorentz factor, in our geometry equal to $(\sin 2\theta \sin \theta)^{-1}$; P the polarization factor $1 + \cos^2 2\theta \cos^2 2\theta_m$, $2\theta_m$ being the monochromator reflection angle; F the structure factor of the unit cell, for superstructure lines equal to $(f_{Ni} - f_{Fe})$, for fundamental lines to $3f_{Ni} + f_{Fe}$; n the multiplicity factor, i.e., the number of equivalent $\{hkl\}$ planes; and D the Debye-Waller factor $\exp[-16\pi^2 \sin^2 \theta \Delta X^2/(3\lambda^2)]$, where ΔX^2 is the mean-square thermal displacement of the atoms (differences between Ni and Fe being neglected).

III. SPECTRUM ANALYSIS

For a binary A-B alloy the maximum information about atomic order, obtainable with scattering methods, is a complete set of Warren-Cowley short-range-order parameters[26] $\alpha_{lmn} = 1 - p_{BA}^{lmn}/c_A$. In a central approximation, $p_{BA}^{(i)}$ is the fraction of A atoms in shell i around an arbitrary B atom, and c_A is the concentration of A atoms. The alloy is said to be long-range ordered if α_i has constant nonzero values for large shell radii. When in a long-range-ordered alloy two types of sublattices can be distinguished, α for A atoms and β for B atoms, the long-range-order parameter is defined as $\eta = w_{A\alpha} - w_{A\beta}$. Here $w_{A\alpha}$ and $w_{A\beta}$ are site probabilities: $w_{A\alpha}$ is the fraction of α sites, occupied by A atoms, and $w_{A\beta}$ is defined similarly. In a stoichiometric A_3B alloy with the Ll$_2$ structure $\eta = 4(w_{A\alpha} - \frac{3}{4})$ and, as shown by Cowley,[26] $\alpha_{odd} = -\frac{1}{3}\eta^2$ and $\alpha_{even} = \eta^2$ for large shell radii.

Clearly, with scattering methods the average number $\bar{n}_i$ of A atoms in shell i (containing z_i atoms) around a B atom can be detected: $\bar{n}_i = z_i p_{BA}^{(i)} = z_i c_A(1 - \alpha_i)$. Naturally the number of A atoms will be distributed around this average value with certain probabilities $w_n^{(i)}$: $\bar{n}_i = \sum_n n w_n^{(i)}$. Starting from a set of α_i parameters, there is however no direct way to determine the $w_n^{(i)}$. Several newer experimental techniques, based on nuclear hyperfine interactions (notably NMR and ME), in principle, are capable of doing so. But the limited resolution usually prevents observations further than the second-neighboring shell. For the same reason the spectra often can be analyzed only by assuming beforehand a certain distribution $w_n^{(i)}$, with $\bar{n}_i$ to be fitted. Schwartz and Asano[27] recently criticized the practice, frequently followed in the literature[21, 28-30] of calculating the $w_n^{(i)}$ for a particular α_i value by assuming a binomial distribution of the numbers n. This distribution implies that the occupational probabilities of the sites in a particular shell are independent of each other, and this only is true in a completely disordered alloy (all $\alpha_i = 0$).

For long-range-ordered alloys a better approximation of the $w_n^{(i)}$ is obtained from the site probabilities w calculated from η. Then we know the numbers of A and B atoms on the sublattices. At this stage we assume that the wrongly placed atoms are distributed at random over the sites in the "wrong" sublattices. This is equivalent to saying that—in addition to the short-range order which arises from the long-range order—no extra short-range order is present. In a stoichiometric A_3B alloy with the Ll$_2$ structure each β site is surrounded in its first shell by 12 α sites, but each α site by four β and eight α sites. The
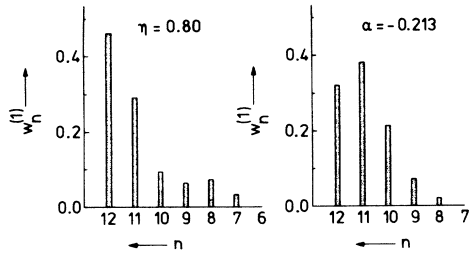
FIG. 2. Probability $w_n^{(1)}$ of having n Ni atoms around a central Fe atom in the first-neighboring shell, calculated with the long- and the short-range-order parameters (η and α, respectively).

probability of finding $n\,A$ atoms in the first shell around an arbitrary B atom can be written

$$w_n^{(1)} = w_{BB}P_{12}(w_{A\alpha}, n)$$

$$+ (1 - w_{BB}) \sum_{m=0}^{4} P_4(w_{AB}, m)P_8(w_{A\alpha}, n-m) , \quad (1)$$

where $P_i(w, j)$ stands for the binomial distribution

$$[i! / j! (i-j)!] w^j (1-w)^{i-j} ,$$

and the number m evidently is restricted to values with $0 \leq n - m \leq 8$. In Fig. 2 the difference between distribution (1) (left-hand plot) and the above-mentioned single binomial distribution[21] (right-hand plot) is illustrated. The probabilities $w_n^{(1)}$ are plotted for different n, the number of Ni atoms in the first shell around a central Fe atom. The $w_n^{(1)}$ have been calculated for $\eta = 0.8$, which corresponds to $\alpha_1 = -\frac{1}{3}\eta^2 = -0.213$; in both cases $\bar{n}_1 = 10.92$, as it should be. In the right-hand plot the "wrongly" situated Fe atoms with about 8 Ni neighbors are clearly absent. In this context we mention that in the Refs. 20 and 31 the "wrongly" situated Ni and Fe atoms, respectively, were not taken into account.

We only analyzed the profiles of the two outer Mössbauer lines because the four inner lines did not show sufficient structure (cf. Fig. 3). It appeared that the first- and second-neighboring shells were sufficient for the analysis. The lines were fitted with a sum of Lorentzians, corresponding to the possible atomic configurations, and weighed in accordance with their respective probabilities. The probability of a certain configuration with n_1 Fe atoms in the first, and n_2 Fe atoms in the second shell around an arbitrary Fe atom is given by the product of $w_{12-n_1}^{(1)}$ and $w_{6-n_2}^{(2)}$, where $w^{(1)}$ has been given above and $w^{(2)}$ is the distribution for the second shell with 6 atoms. A table of values for different long-range-order parameters can be found in Ref. 24. Configurations with the same numbers n_1 and n_2 but with
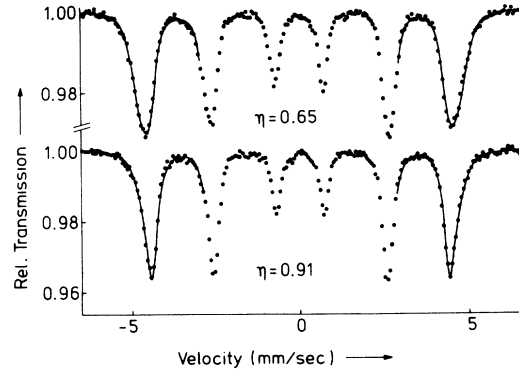
FIG. 3. Room-temperature spectra of two Ni_3Fe samples with different degrees of order. The solid lines represent the computer fits for the indicated values of η.

different spatial orientations were assumed to give identical hyperfine interactions. Further assumptions, necessary for the analysis, are the following: (a) the hyperfine field is linearly related to n_1 and n_2: $|H_{hf}| = H(0, 6) + n_1\Delta H_1 + (n_2 - 6)\Delta H_2$; (b) the isomer shift is proportional to n_1; (c) anisotropic interactions can be neglected. $H(0, 6)$ is the absolute value of the field in the fully ordered alloy with $n_1 = 0$ and $n_2 = 6$. The position P of the outer lines of the subspectra are now given by

$$P = IS(0) + n_1\Delta IS \pm \tfrac{1}{2}|H_{hf}| .$$

$IS(0)$ is here the isomer shift for a ^{57}Fe nucleus with zero Fe neighbors and ΔIS is the change in isomer shift for each extra Fe neighbor. All linewidths were held equal in the analysis. In order to prevent interference of the outer lines one and six with the inner lines two and five, which show some overlap in several spectra, the outer flanks of lines two and five each were fitted with two dummy lines.

IV. RESULTS AND DISCUSSION

A. ME measurements

As a first step, all spectra were analyzed as broadened six-line patterns. The relevant parameters of these fits are compiled in Table I, together with the annealing treatments of the foils. The isomer shift (IS), which is calculated for a Ni_3Fe source relative to an Fe absorber, stays close to the value of -0.02 mm sec^{-1} found for Fe as an impurity in Ni metal. We also tabulated the average width Γ of the outer lines. The spectra of the foils $A2$ and $A9$ are depicted in Fig. 3. We see that the widths of the inner lines are considerably smaller than those of the outer lines. This indicates a magnetic, instead of an electrostatic, interaction difference for Fe atoms in dif-

TABLE I. Annealing treatments and single line fits of room-temperature Ni_3Fe spectra. In the column "Annealing time," the + sign means that the preceding time has to be added. From the spectrum parameters only the isomer shift (IS), the width of the outer lines (Γ), and the average hyperfine field $|\bar{H}_{hf}|$ are given. Experimental errors are placed in parentheses.

Foil No.	Annealing temp (K)	Annealing time (h)	IS (mm/sec) (± 0.01)	Γ (mm/sec) (± 0.01)	$|\bar{H}_{hf}|$ (kOe) (± 0.3)
A1	As rolled		−0.02	0.75	295.7
A2	760	16	−0.01	0.67	286.5
A3	760	38.5	−0.01	0.62	284.9
A4	760	83.5	0.00	0.53	282.6
A5	760	153	0.00	0.53	281.2
A6	760	266	0.00	0.52	280.7
A7	700	+118	0.00	0.50	279.3
A8	700	214	+0.01	0.49	279.0
A9	633	+137	+0.01	0.45	278.0
A10	633	303	+0.01	0.45	278.7
B1	As rolled		−0.03	0.86	294.3
B2	760	21.5	−0.01	0.65	286.2
B3	760	48	−0.01	0.64	283.9
B4	760	90.5	0.00	0.54	281.2
B5	760	183.5	0.00	0.49	281.3
B6	760	300.5	0.00	0.49	279.7
B7	691	+158	+0.01	0.47	280.2
B8	691	371	−0.01	0.47	280.0
B9	622	+150.5	0.00	0.45	279.1
B10	622	250	0.00	0.46	278.0

ferent surroundings, so that Γ is related to the hyperfine field distribution in the sample, as assumed in Sec. III. Upon ordering the mean field approaches the value of 272 kOe, which is observed for Fe as impurity in Ni metal.[32] The quadrupole shift was nearly zero for all spectra, as expected for a cubic alloy in a six-line analysis. The similarities in H_{hf} and IS of ordered Ni_3Fe and Ni metal suggest that the first-neighboring shell largely determines the hyperfine parameters in these metals.

As a second step, the profiles of the outer lines were analyzed as described in Sec. III for different values of η. The well-ordered foils (A6−A10 and B5−B10) exhibited a pronounced dip in their χ^2-vs-η curves. Also the spreads in the values of ΔIS, $H(0, 6)$, ΔH_1, and ΔH_2 were small in these foils, giving confidence in the correctness of our starting points. For the less-ordered foils χ^2 was nearly constant for varying η. In order to obtain convergence there we fixed ΔH_2. The fits had been rather insensitive to changes in this parameter, while the other two parameters of interest $H(0, 6)$ and ΔH_1, were strongly correlated. Actually, no large change in ΔH_2 is expected upon ordering, because this parameter describes the influence of the more distant second shell.

So, for all spectra, the analysis was repeated with ΔH_2 fixed at 2.4 kOe, the average value, found for the well-ordered foils in the preceding

analysis. We now obtained distinct minima in the χ^2-vs-η relations for all spectra, except the disordered A1 and B1. The results, corresponding to the lowest χ^2 values (χ^2 has expectation value 1), are presented in Table II. For the foils A1 and B1 the parameter values for $\eta = 0$ are tabulated, though for $\eta \neq 0$ a lower χ^2 was found. These two foils will be discussed below. The solid lines in Fig. 3 represent the fits obtained for the spectra of A2 and A9. The final values of the parameters averaged over all foils except A1 and B1 are ΔIS = +0.008(1) mms^{-1}, $H(0, 6)$ = 276.5(2) kOe, ΔH_1 = +10.7(2) kOe, and ΔH_2 = +2.4(1) kOe, the standard deviations in the last decimal numbers being placed in parentheses. We note that the change of H_{hf} with iron concentration in disordered Ni-Fe alloys between 0 and 50% Fe can be described with nearly the same hyperfine field parameters.[33] This once more stresses the local character of the hyperfine interactions in these alloys.

The adopted procedure for the line-profile analysis appears to work quite well. The linewidths of the subspectra for instance, which are not tabulated but have an average value of 0.32 mm sec^{-1}, are close to the experimental width of 0.28 mm sec^{-1}. An abnormal small width would indicate that too many parameters had been used in the analysis. Also ΔIS, $H(0, 6)$, and ΔH_1 remain constant over the range $\eta = 0.6-0.9$. Apart from confirming that the hyperfine field distribution de-

TABLE II. Multiline fits of room-temperature Ni₃Fe spectra with parameter ΔH_2 fixed at 2.4 kOe. For the disordered foils $A1$ and $B1$ only $\eta = 0$ was used. The symbols in the column headings are explained in the text. Standard deviations of the average values are placed in parentheses.

Foil No.	χ^2	η	IS(0) (mm/sec)	ΔIS (mm/sec)	$H(0,6)$ (kOe)	ΔH_1 (kOe)
$A1$	2.25	0.00	−0.04	+0.007	272.4	12.1
$A2$	1.23	0.63	−0.03	+0.009	275.5	11.2
$A3$	1.14	0.70	−0.02	+0.006	276.7	10.6
$A4$	1.68	0.78	−0.01	+0.005	277.2	10.3
$A5$	1.48	0.80	−0.01	+0.010	276.5	10.3
$A6$	2.61	0.86	−0.01	+0.007	277.6	11.3
$A7$	1.36	0.87	−0.01	+0.014	276.6	11.5
$A8$	1.93	0.88	0.00	+0.011	276.8	11.1
$A9$	1.14	0.87	0.00	+0.005	275.3	11.3
$A10$	1.27	0.89	0.00	+0.011	276.5	11.5
Average values A series:				+0.009	276.5	11.0
(Except foil $A1$)				(±0.001)	(±0.3)	(±0.2)
$B1$	2.25	0.00	−0.04	+0.005	271.5	11.6
$B2$	1.21	0.67	−0.03	+0.007	276.8	10.8
$B3$	1.30	0.71	−0.02	+0.007	276.0	10.6
$B4$	1.68	0.78	−0.01	+0.005	276.2	10.3
$B5$	2.50	0.83	0.00	+0.006	277.6	10.6
$B6$	2.28	0.84	−0.01	+0.006	276.3	10.3
$B7$	1.71	0.83	0.00	+0.003	276.9	9.4
$B8$	1.41	0.86	−0.01	+0.009	277.2	10.9
$B9$	2.26	0.88	−0.01	+0.007	276.8	10.0
$B10$	1.03	0.86	0.00	+0.008	275.3	10.7
Average values B series:				+0.006	276.6	10.4
(Except foil $B1$)				(±0.001)	(±0.2)	(±0.2)

pends exclusively on the numbers n_1 and n_2, this result shows that ΔH_1 is independent of n_1 from $n_1 = 0$ up to $n_1 = 3$. The probability of more than three atoms in the first shell is too small to detect a possible deviation from linearity. Further it seems reasonable that ΔH_2 is smaller than ΔH_1. In order to investigate the outcome of the fitting procedure when the second-shell contribution is fully neglected, three spectra were analyzed with $\Delta H_2 = 0$. We observed (see Table III) poorer reproducibility in the parameter values and a significant increase in χ^2. In one case ($B8$) no convergence could be obtained. Therefore we concluded that two shells are necessary for a meaningful analysis.

We also checked the possibility of line broadening by an anisotropic hyperfine field and/or an electric field gradient. Indeed the relations between the linedepths in the single-line fits of the less-ordered foils (cf. Fig. 3) show the existence of some quadrupolar lineshift in the subspectra. For several atomic configurations this type of broadening must be absent. This for instance, is the case when an iron atom occupies a lattice site with a (0, 6) environment (typical for the fully ordered lattice), which has cubic point symmetry. Neither can an effect be expected for an iron atom at a nickel site in an otherwise ordered lattice. Then the angle θ between the direction of the hyperfine field ($\langle 111 \rangle$ in ordered Ni₃Fe) and the main axis of the anisotropic-field and/or electric-field-gradient tensor is such that $\cos^2\theta = \frac{1}{3}$, leading to zero line shift. For several spectra the analysis was repeated with two linewidth parameters, one assigned to the cases mentioned above, for which line broadening must be absent, and the other assigned to all other cases. However, there existed no correlation between type of lattice site and linewidth, so that we concluded that anisotropic interactions are negligible in Ni₃Fe, with exception of a small effect in the disordered alloy. This is in contrast with results for ordered NiFe.[34]

Our method of analysis is not conclusive with respect to the cold-rolled foils $A1$ and $B1$. As shown in Table II, these foils fit in the complete alloy series if η is fixed at 0. But when η is released, a minimum χ^2 is found at the rather high value of $\eta = 0.65$. Yet the average hyperfine fields $\bar{H}_{hf}$ of $A1$ and $B1$, as determined with the six-line analysis, are only consistent with our model when these foils have a low longe-range order. This is demonstrated by a plot of $\bar{H}_{hf}$ vs η^2. Because in our approach η^2 is proportional to α_1 and α_2 (see Sec. III), and thus proportional to the average numbers $\bar{n}_1$ and $\bar{n}_2$, and because H_{hf} is linearly related to n_1 and n_2, $\bar{H}_{hf} \sim \eta^2$. This relation, calculated with the values obtained for $H(0, 6)$, ΔH_1, and ΔH_2, is plotted in Fig. 4 as a dashed line. In the same figure the measured $\bar{H}_{hf}$ values from Table I are indicated. We see that the field values of the cold-worked foils—here depicted for an assumed value $\eta = 0$—are only consistent with the

TABLE III. Multiline fits of three spectra in a one-shell model, taking $\Delta H_2 = 0$ kOe. For comparison the χ^2 and η values from the two-shell analysis are also tabulated.

Foil No.	χ^2 (Two shell)	η (Two shell)	χ^2 (One shell)	η (One shell)	IS(0) (mm/sec)	ΔIS (mm/sec)	$H(0,6)$ (kOe)	ΔH_1 (kOe)
$B3$	1.30	0.71	1.50	0.62	−0.02	+0.006	271.5	8.3
$B8$	1.41	0.86	1.45	0.73	−0.01	+0.004	273.3	6.4
$B9$	2.26	0.88	2.42	0.77	−0.01	+0.004	273.8	5.8
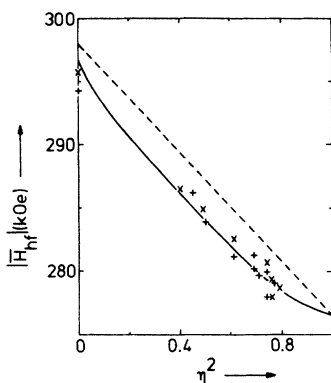
FIG. 4. Relation between $\overline{H}_{hf}$ and η^2. Indicated are the experimental values for foil series A (+) and B (x). The dashed line represents the theoretical $H_{hf} \sim \eta^2$ relation. The solid line represents the same, but with instrumental effects included.

FIG. 5. Relation between Γ and η^2: (x) experimentally determined; or (●) calculated from simulated spectra.

other field values for a low degree of order.

The observed deviation of the experimental H_{hf} values from the calculated line is only an artifact, created by different definitions of the two average fields: the calculated field is a true average, while the experimental field is obtained from single-line fits of composite lines. The definitions will only yield the same answer if the field distribution is symmetric around the average value, which is not the case here. For a more exact treatment we simulated spectra for different η and performed single-line fits of the outer lines. The hyperfine fields obtained are plotted in Fig. 4 as a solid line. The seeming discrepancy is removed and we conclude that the average fields of the disordered foils fit in our model. We also plotted the Γ values of the simulated spectra, together with the experimental linewidths (see Table I), against η^2 (see Fig. 5). For all partly ordered alloys the experimental Γ is in accordance with the expected value. This result shows that the ordering reaction at 760 K did proceed homogeneously, since otherwise extra line broadening would occur, due to the presence of a two-phase mixture. The character of the order-disorder reaction is discussed further in the ensuing paper.

The reason that the line-profile analysis did not succeed for the disordered foils may be found in the special microstructure of a cold-rolled foil. A close investigation of foils, disordered through ultrarapid quenching, is required to clear up this point. We may mention here a preliminary result, obtained from a sample which was quenched from 1300 K to RT with 5×10^4 K sec^{-1}. Average hyperfine field and linewidth (294 kOe and 0.87 mm sec^{-1}, respectively) were in concurrence with the data from the cold-rolled foils. Unfortunately, the foil
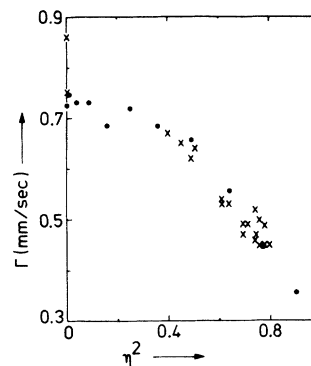
was too thick for a line-profile analysis.

The solid line in Fig. 4 can be used as a calibration for the long-range-order parameter in terms of the average hyperfine field, measured at room temperature. As an alternative we performed a least-squares fit to the measured points (except $A1$ and $B1$), assuming a linear relationship between $\overline{H}_{hf}$ and η^2:

$$\eta^2 = A(H_{hf} - 281.14) + B .   (2)$$

Inspection of Fig. 4 shows that this will be a good approximation for $\eta \lesssim 0.9$. The fit was performed with the field values of $\overline{H}_{hf}$ relative to their average value of 281.14 kOe in order to obtain independent A and B parameters. We obtained $A = -0.045(3)$ kOe^{-1} and $B = +0.658(8)$, the standard deviations in the last decimal numbers being placed in parentheses. When we neglect the measuring errors in $\overline{H}_{hf}$, we may attribute the spread in the points of Fig. 4 to errors in the determination of η, introduced by the line-profile analysis. We find then from the sum of the square deviations a standard deviation $\sigma(\eta) = 0.02$, being the average error in the determination of η with the line-profile analysis. Finally, because the coefficients A B are independent, we can calculate the accuracy of the calibration (2). In the interval $0.65 \leqslant \eta \leqslant 0.90$ the standard deviation of the predicted value of η is smaller than 0.02.

B. X-ray measurements

For a comparison of Mössbauer-effect and x-ray diffraction results we measured the intensities of the 100 and 200 Debye-Scherrer lines from the foils $B1$ and $B6-B9$. A strong (100) texture became evident from a 50 fold increase in the intensity ratio of the 200 and 111 lines. This texture is known to be introduced in fcc Ni-Fe alloys through cold rolling. Owing to this enhancement the statistical error in the 100 intensity was be-

TABLE IV. X-ray data for the foils $B6-B9$: intensity ratio I_{100}/I_{200}, x-ray value for η, Mössbauer value for η, and domain size d.

Foil No.	I_{100}/I_{200}	η (x ray)	η (Mössb.)	d (Å)
$B6$	0.0154	0.80	0.84	160
$B7$	0.0172	0.85	0.83	160
$B8$	0.0174	0.85	0.86	170
$B9$	0.0169	0.84	0.88	170

low 0.5%, the border set by the long-term instrumental stability. The grain size of the foils (which were not recrystallized after cold rolling) was estimated from the width of the fundamental lines by comparison with well-recrystallized silicon, and amounted to several tenths of a micron. Therefore extinction effects are thought to be negligible.

As expected, the 100 intensity was zero for the disordered $B1$ foil. The pertinent data for the other foils $B6-B9$ are presented in Table IV. First η was calculated in a straightforward manner, using the atomic scattering factors f_{Ni} and f_{Fe} calculated by Doyle and Turner[35] and the dispersion corrections of Cooper.[36] The Debye-Waller factor was taken into account with a 4% correction of I_{200}, taken from the work of Calvayrac and Fayard.[10] We then obtained improbably high values for η between 0.95 and 1.01. However, Calvayrac and Fayard observed in Ni_3Fe 100 intensity which was a factor 1.41 higher than expected on basis of the calculated scattering factors. The values of η, obtained after this effect is taken into account, are given in the column η (x-ray) of Table IV. Unfortunately, I_{300} was too low for a quantitative analysis.

The origin of the enhancement of the 100 line has to be found in an abnormal behavior of the atomic scattering factors of Ni and Fe at low scattering angles. One of the possible mechanisms, mentioned by Calvayrac and Fayard, can be ruled out on basis of our ME results. It concerns the transfer of 0.3 electron charge from the iron atoms to each nickel atom. The resulting charge difference of 1.2 unit charge between Ni and Fe would account for the larger $(f_{Ni} - f_{Fe})$ value, but also cause an electric field gradient at the iron nucleus, which, as discussed above, is not observed.

The Mössbauer values η(Mössbauer) are listed next to the column η(x-ray) in Table IV. On the average they are 0.02 higher than the corresponding x-ray results. In the last column the

average domain size d is found, as determined from the width of the superstructure lines with the Scherrer formula. We think that the domain size is restricted by lattice imperfections, present in the cold-rolled foils, and that this explains the constant value of d.

When comparing η(x-ray) and η(Mössbauer), we have to realize that x-ray diffraction measures the true long-range order, while the hyperfine field is only sensitive to the occupation of the first- and—to a much lesser extent—the second-neighboring shell. Therefore η(Mössbauer) can be put equal to $(-3\alpha_1)^{1/2}$, where α_1 is the short-range-order parameter of the first shell as defined in Sec. III. The question is whether η(Mössbauer) is equal to the true η, or that there exists a considerable amount of extra first-shell order above the α_1 associated with the long-range order. In the most thoroughly studied ordered alloy (Cu_3Au) this question seems not to be settled, as illustrated by the different interpretations given by Schwartz and Cohen,[37] Gantois,[38] and Morris,[39] of their respective results. For Ni_3Fe, we find an average difference of only 0.02 between η(x-ray) and η(Mössbauer), which is within our experimental uncertainty. A more comprehensive study of this question seems desirable.

V. CONCLUSIONS

We have shown that the ME technique, by means of a line-profile analysis, is capable of measuring atomic order in Ni_3Fe. It appears that the hyperfine field in partly ordered Ni_3Fe is linearly related to the numbers of Fe atoms in the first and second shell around a ^{57}Fe nucleus, and that anisotropic hyperfine interactions are small. For alloys with $\eta \leq 0.9$ the average hyperfine field at room temperature, obtained from single-line fits of the outer lines, is linearly dependent on η^2 and can be used to determine the long-range-order parameter η. For several foils, η was also measured with the x-ray diffraction technique. The abnormal atomic scattering factors of Ni and Fe atoms at low scattering angles are shown not to be caused by charge transfer. The ME and x-ray results for η are in accordance with each other, indicating that not much short-range order exists in addition to that arising from the long-range order. A closer examination of this point is however necessary.

*Present address: Technical Physics Department, Experimental Physics Laboratory, Univ. of Utrecht, Utrecht, The Netherlands.

[1] R. M. Bozorth, Rev. Mod. Phys. 25, 42 (1953).

[2] S. Chikazumi and C. D. Graham, Jr., in *Magnetism and Metallurgy*, edited by A. E. Berkowitz and F. Kneller (Academic, New York, 1969), p. 580.

[3] R. J. Wakelin and E. L. Yates, Proc. Phys. Soc. Lond. B 66, 221 (1953).

[4] R. G. Davies and N. S. Stoloff, Acta Metall. 11, 1347 (1963).

[5] M. F. Collins, R. V. Jones, and R. D. Lowde, J. Phys. Soc. Jpn. Suppl. 17, 19 (1962); M. F. Collins and J. B. Forsyth, Philos. Mag. 8, 401 (1963).

[6] V. I. Goman'kov, I. M. Puzei, and A. A. Loshmanov, Kristallografiya 10, 416 (1965) [Sov. Phys.-Crystrallogr. 10, 338 (1965)]; Fiz. Met. Metalloved. 22, 128 (1966) [Phys. Met.-Metallogr. 22, 134 (1966)]; V. I. Goman'kov, I. M. Puzei, and M. N. Rukosuev, Kristallografiya 13, 543 (1968) [Sov. Phys.-Crystrallogr. 13, 449 (1968)].

[7] J. W. Cable and E. O. Wollan, Phys. Rev. B 7, 2005 (1973).

[8] R. G. Treuting and B. W. Batterman, J. Appl. Phys. 34, 2005 (1963).

[9] W. L. Wilson and R. W. Gould, J. Appl. Crystallogr. 5, 125 (1972).

[10] Y. Calvayrac and M. Fayard, C. R. Acad. Sci. C 275, 1 (1972).

[11] E. Josso, J. Phys. Radium. 12, 399 (1951).

[12] S. Iida, J. Phys. Soc. Jpn. 9, 769 (1955).

[13] A. E. Vidoz, D. P. Lazarević, and R. W. Cahn, Acta Metall. 11, 17 (1963).

[14] Y. Calvayrac and M. Fayard, Phys. Status Solidi A 17, 407 (1973).

[15] C. F. Varotto and A. E. Vidoz, J. Mater. Sci. 6, 294 (1971).

[16] Y. Calvayrac and M. Fayard, Mater. Res. Bull. 7, 891 (1972).

[17] R. J. Taunt and B. Ralph, Phys. Status Solidi A 24, 207 (1974).

[18] T. G. Kollie and C. R. Brooks, Phys. Status Solidi A 19, 545 (1973).

[19] U. Erich, Z. Phys. 227, 25 (1969).

[20] T. J. Burch, J. I. Budnick, and S. Skalski, Phys. Rev. Lett. 22, 846 (1969).

[21] A. Heilmann and W. Zinn, Z. Metallkd. 58, 113 (1967).

[22] J. Poláková, J. Lauermannová, and T. Zemčik, Proceedings of the Fifth International Conference on Mössbauer Spectroscopy, Bratislava, 1974, edited by M. Hucl, and T. Zemčík, p. 298 (unpublished).

[23] A preliminary report has been given in J. Phys. (Paris) Colloq. 35, C 6-347 (1974).

[24] J. W. Drijver, Ph.D. thesis (University of Groningen, 1975) (unpublished).

[25] A. Guinier, *X-ray Diffraction* (Freeman, San Francisco, 1963); B. E. Warren, *X-ray Diffraction* (Addison-Wesley, Reading, Mass., 1969).

[26] J. W. Cowley, Phys. Rev. 77, 669 (1950); 120, 1648 (1960); *Diffraction Physics* (North-Holland, Amsterdam, 1975).

[27] L. H. Schwartz and A. Asano, J. Phys. (Paris) Colloq. 35, C 6-453 (1974).

[28] O. Brümmer, G. Dräger, and I. Mistol, Ann. Phys. (N.Y.) 28, 135 (1972).

[29] S. J. Campbell and T. J. Hicks, J. Phys. F 5, 27 (1975).

[30] J. Ray and G. Chandra, Solid State Commun. 19, 101 (1976).

[31] M. Kanashiro and N. Kunitomi, Solid State Commun. 19, 1127 (1976).

[32] M. Hucl (unpublished).

[33] J. W. Drijver and F. van der Woude, J. Phys. (Paris) Colloq. 37, C6-385 (1976).

[34] L. Billard and A. Chamberod, Solid State Commun. 17, 113 (1975).

[35] P. A. Doyle and P. S. Turner, Acta Crystallogr. A 24, 390 (1968).

[36] M. J. Cooper, Acta Crystallogr. 16, 1067 (1963).

[37] L. H. Schwartz and J. B. Cohen, J. Appl. Phys. 36, 598 (1965).

[38] M. Gantois, J. Appl. Crystallogr. 1, 263 (1968).

[39] D. G. Morris, Phys. Status Solidi A 32, 145 (1975).

FIG. 2. Probability $w_n^{(1)}$ of having n Ni atoms around a central Fe atom in the first-neighboring shell, calculated with the long- and the short-range-order parameters (η and α, respectively).